DEU FMD 27(79) (2025) 62-71

Dokuz Eylül Üniversitesi Mühendislik Fakültesi Fen ve Mühendislik Dergisi
Dokuz Eylul University Faculty of Engineering Journal of Science and Engineering
Elektronik/Online ISSN: 2547-958X

RESEARCH ARTICLE / ARAŞTIRMA MAKALESI

An Adaptive PI Controller Design for Current Control of Brushless DC Motor Drives

Fırçasız Doğru Akım Motor Sürücülerinin Akım Kontrolü için Bir Uyarlamalı PI Kontrolcü Tasarımı

Ceyhun Arslanoğlu *, **Fatih Adıgüzel**

Yıldız Technical University, Faculty of Electrical and Electronics, Department of Control and Automation Engineering, İstanbul, TÜRKİYE
Corresponding Author / Sorumlu Yazar *: ceycanarslanoglu@gmail.com

Abstract

Brushless direct current motor(BLDCM) are used to drive many systems in numerous fields. The control of BLDCM with basic drive techniques is required to obtain the desired output. Although basic drive techniques may be unsatisfactory in meeting these demands, they have found an invariable place for themselves due to their easy-to-use advantages. Due to these reasons, many researchers have focused on how innovative solutions are developed. In this paper, an adaptive PI controller is proposed to control the current of BLDCM drives. This paper aims to design a PI controller with time-varying gains for current regulation. The adaptive PI, improving the steady-state response, is constructed by one adaptation rule and a classical PI. In addition, the stability analysis is proved with Lyapunov theory. To demonstrate the effectiveness of the proposed controller, several simulations are performed with comparisons. The simulations with a classical PI and high-gain current controller comparisons are presented for set-point and sinusoidal references, and 500 rpm and 1500 rpm motor speeds. Comparing the classical PI with adaptive controller, the adaptive controller improves the current performance from 0.3442 to 0.0656 for 500 rpm, and from 0.4703 to 0.1552 for 1500 rpm in RMS of the current errors for 2A reference current. Similarly, the outcomes of comparing the high-gain controller to the adaptive PI show that the designed controller reduces RMS of the currents errors from 0.1853 to 0.1611 for 1500 rpm with 2A reference current, and from 0.1879 to 0.1720 for 1500 rpm with a sinusoidal reference current.

Keywords: *Brushless direct current motor drives, Adaptive control, PI controller, Current control*

Öz

Fırçasız doğru akım motoru(FDAM), sayısız alanda birçok sistemi tahrik etmek için kullanılmaktadır. FDAM temel tahrik teknikleriyle kontrolü, istenilen performansın alınabilmesi için gereklidir. Her ne kadar klasik yaklaşımlar bu talepleri karşılamada yetersiz kalsa da klasik kontrolörler kolay sürüş avantajlarından dolayı kendilerine değişmez bir yer bulmuşlardır. Bu nedenlerden dolayı, birçok araştırmacı yenilikçi çözümlerin nasıl geliştireceği üzerine odaklanmıştır. Bu makalede, FDAM akım kontrolü için uyarlamalı bir PI kontrolcü önerilmektedir. Bu makaledeki amaç, FDAM akım regülasyonu için zamanla değişen kontrolör kazançlarına sahip bir PI kontrolcü tasarlamaktır. Sürekli rejim yanıtını iyileştiren önerilen uyarlamalı PI kontrolcü, bir uyarlama kuralı ve klasik bir PI kontrolcüden oluşmaktadır. Ayrıca, kararlılık analizi Lyapunov teorisi ile kanıtlanmıştır. Önerilen kontrolörün etkinliğini göstermek için karşılaştırmalarla çeşitli simülasyonlar gerçekleştirilmiştir. Klasik PI ve yüksek kazançlı akım kontrolörü ile yapılan benzetimler, sabit ve sinüzoidal referanslar ile 500 rpm ve 1500 rpm motor hızları için karşılaştırmalı olarak sunulmuştur. Klasik PI, uyarlamalı kontrolcü ile karşılaştırıldığında, uyarlamalı kontrol 2A referans akımı için akımlarının hatasının RMS'deki akım performansını 500 rpm hız için 0,3442'den 0,0656'ya ve 1500 rpm hız için 0,4703'ten 0,1552'ye iyileştirmektedir. Benzer şekilde, yüksek kazançlı kontrolcünün uyarlamalı PI ile karşılaştırma sonuçlarında, uyarlamalı kontrolcü, motor akımlarının hatasının RMS'sini 2A referans akımında 1500 rpm hız için 0,1853'ten 0,1611'e ve sinüzoidal referans akımında 1500 rpm hız için 0,1879'dan 0,1720'ye düşürmektedir.

Anahtar Kelimeler: *Fırçasız doğru akım motor sürücüsü, Uyarlamalı kontrol, PI kontrol, Akım kontrol*

1. Introduction

A brushless direct current motor (BLDCM) is an electric motor, which is supplied by a DC voltage source and is commutated electronically without using of any brushes, unlike the conventional DC motor. The definition of BLDCM types is simplified as PMSMs having the trapezoidal-induced emf are known as permanent magnet brushless direct current motors (PMBLDCM) [1]. In recent years, due to its many advantages, such as simple structure, high efficiency, large torque, etc., BLDCM drives have been a viable option in industries like robotics, aerospace, industrial process control, household appliances, and more [2, 3]. Unlike conventional DC motors, PM brushless DC motors are commutated electrically. Thus, it requires continuous information on the rotor position to rotate the motor.

Over the years many control methods have been employed for the control of BLDC motor drives. Due to the fact that BLDC motor is a permanent magnet synchronous motor, vector control methods such as field-oriented control (FOC) [4] and direct

DOI: https://doi.org/10.21205/deufmd.2025277909

Geliş Tarihi / Received: 27.12.2023
Kabul Tarihi / Accepted: 16.04.2024

torque control (DTC) [5], have been quite popular methods. The control of BLDCM drives requires continuous information on the rotor position. However, this can be overwhelming in terms of costs. Therefore, some sensor-less methods including Kalman Filter [6] and Model Predictive Control (MPC) [7], have been employed to that FOC [8], DTC and many other control methods like back-EMF difference estimation methods [9, 10, 11] and back-EMF zero cross detection estimation [12] to exclude the sensors. Each of these methods has its advantages and disadvantages. However, none of them has the simplicity of a classical PI/PID controller.

The PID has been widely used since its introduction in the 1940s during the analog era. Examples of modern digital systems that utilize it include distributed control systems (DCS), supervisory control and data acquisition (SCADA), and digital systems [13]. As the systems advanced through the years, the need for tuning methods was brought along, such as Ziegler-Nichols. Having a simple structure and easy-to-use advantages have made PI/PID controllers be employed in many kinds of systems. However, systems in real life have nonlinearities and uncertainties, which need to be dealt with by an advanced controller. Although Ziegler-Nichols is simple and intuitive, it lacks good stability margins and creates a closed-loop system that is poorly damped. Hence, conventional PID controller struggles to adapt to varying operating conditions, leading to suboptimal performance. To overcome this problem, advanced methods, which are aforementioned, were brought up, implemented, and tested. The outcome of these advanced control methods has shown better performance in terms of trajectory tracking and compensation of nonlinearities, disturbances and even varying load conditions than a conventional PID controller. However, these advanced control methods are quite complicated in structure, and in the sense of computation, they are rather expensive and overwhelming. In practice, to reduce the cost and computational burden, these advanced methods have been undesired. As long as the PI/PID controller can compensate for the effects of nonlinearities, uncertainties parameter variations, etc., it will be the go-to choice for many systems. The synthesis of a universal PI control for nonlinear systems with analytically calculated gains, while guaranteeing stability and transient performance, is an ongoing unresolved topic. If the systems contain actuation failures, external disturbances, and modeling uncertainty, the issue becomes even more complex [14]. Multiple methods have been implemented for the control of nonlinear systems ranging from linearization of nonlinear systems into a linear system, adaptive backstepping control [15], to direct compensation of nonlinear systems by integrating neural networks (NN) with approximation capabilities [16]. Moreover, in [17] with the implementation of feedback linearization, an equivalent linear system for a DC motor was obtained and controlled with a linear quadratic regulator (LQR) to improve the performance. Furthermore, in [18] an adaptive input-output feedback linearization control, which was robust against the variation of motor parameters, for a non-ideal BLDC motor is proposed to generate the reference voltages for three phase voltage source inverter (VSI). In [19], an adaptive deadbeat controller using particle swarm optimization (PSO) and an adaptive neuro-fuzzy interference system (ANFIS) were used collaboratively to achieve a deadbeat response. In [20, 21, 22], fuzzy-based PI/PID controllers have been designed and implemented for the control of the speed of BLDC motors, and the incompetency of conventional PI/PID were alleviated in terms of compensating the side effects of nonlinear systems. In [23], for a class of nonlinear systems, a PI adaptive fuzzy controller has been employed, which ensures stability through Lyapunov theory while ensuring stability and robustness under large and fast varying disturbances. These forenamed algorithms, methods, and techniques have made significant improvements in PI/PID's ability to deal with nonlinear systems and to ensure stability and performance for closed-loop systems. However, there is still much to be discovered in terms of affordability, simplicity, and effectiveness. In [24], a self-tuning PID controller, where the gains of the controller were adjusted online. The adaptation mechanism has been designed based on the Lyapunov approach, ensuring the stability of the designed controller. Moreover, PI/PID controllers have been designed for nonlinear systems with possible sensor and actuation faults, where no linearization and approximation were done and stability was ensured through the Lyapunov approach, with control schemes that are simple in structure and computationally affordable [25, 26, 27]. However, such controllers specifically for BLDCM drives have not been come across in literature.

One of the reasons for the torque ripple in BLDCM drives is the commutation torque ripple which arises from the switching of the model dynamics. To handle this problem, several modified PWM methods are used such as the elimination commutation torque ripple of brushless DC motor with minimum commutation time [28], PWM modulation technique without calculation of commutation time [29], the switched current controller with commutation delay compensation [30], the switched adaptive controller [31]. In this paper, because the updating of the controller gains is considered the system dynamics, the reduction commutation torque is met without an additional controller modification.

The main purpose of this paper is to design an adaptive PI controller to regulate the currents in BLDCM with the elegant presentation of the current model. In the closed-loop nonlinear system containing nonlinearities and uncertainties, the general rule to determine the gains of the PI/PID controller does not exist. The tuning of the controller gains is usually adjusted by the trial-error method and practical concerns in nonlinear systems. However, this paper presents a tuning method for the gain of the PI controller which guarantees that all signals in the closed-loop are bounded aiming that the currents of BLDCM drives regulate in advance. The main philosophy of the structure of the designed controller is first to assign roughly PI controller gains to the BLDCM drives in which the drive is simple but inadequate considering the system performance. Secondly, the system performance is met by time-varying gains of the proposed PI controller which is constructed based on Lyapunov stability despite the system uncertainties, external disturbances, and actuator faults. Finally, the convergence of uniformly ultimately bounded stability of the closed-loop current dynamics is proved in the sense of Lyapunov theory. In addition to the aforementioned advantages of the designed controller, the contributions of this paper can be listed as follows:

1. Although the designed controller for the current control of BLDCM has a fundamental structure, an adaptation rule is employed for the control of the current of BLDCM as if advanced PI controller gains are used in PI control.
2. The controller structure is designed for the control of the conducting period of the motor, however, it is well-known that the BLDCM has a commutation period for each sector of currents. Without an additional controller, the designed controller proceeds due to the adaptation rules in the time-varying controller gain taking into account this switching of system dynamics.

3. The response of the designed controller seems to be a high-gain current controller but it is a controller that consumes less energy and responds easily to a non-linear changing of the system.

To show the effectiveness and viability of the proposed controller, several numerical simulations are carried out by comparing a traditional controller PI and a high-gain controller.

The rest of this paper is organized as follows. In Section 2, some lemmas are introduced to facilitate the understanding of controller design steps in the convergence analysis of the proposed controller. Section 3 gives the dynamic model of the BLDCM drive and its elegant presentation of the implicit current dynamic model. In Section 4, the design steps with the stability analysis of the proposed PI controller are rendered. In Section 5, some computer-based numerical experiments are presented to show the effectiveness of the proposed adaptive controller as to the traditional PI controller and a high-gain current controller. Finally, the conclusions are referred to in Section 6.

2. Preliminaries

This section presents some Lemmas to facilitate the design of the controller to be proposed and the stability analysis of the controller structure.

Lemma 2.1 (Barbalat's Lemma): Let $\alpha(t):[t_0,\infty)\to\mathbb{R}$ be a continuously differentiable scalar function. If $\alpha(t)$ has a finite limit as $t\to\infty$, and $\dot{\alpha}(t)$ is uniformly continuous over $[t_0,\infty)$, then

$$\lim_{t\to\infty}\dot{\alpha}(t)=0. \tag{1}$$

For Proof of Lemma 2.1, see [32].

Consider a PI controller and we define a filtered variable u which is

$$u(t)=e(t)+\beta\int_0^t e(\tau)d\tau. \tag{2}$$

where $e(t)=x(t)-x^*(t)$ is the error of trajectory tracking and $\beta>0$ is a design parameter gain to be determined in the implementation of the controller to be designed for the torque loop control of BLDCM drive. We assume here that $e(t)$ is a sufficiently smooth function.

Lemma 2.2: Consider the filtered variable $u(t)$ given in (2). If $\lim_{t\to\infty}u(t)=0$, then $e(t)$ and $\int_0^t e(\tau)d\tau$ converge asymptotically to zero as $t\to\infty$ with the same decreasing rate with the filtered variable.

Proof: According to Lemma 2.1, it is satisfied that $\lim_{t\to\infty}\dot{u}(t)=0$ which means that

$$\frac{d}{dt}\left(e(t)+\beta\int_0^t e(\tau)d\tau\right)=0. \tag{3}$$

Then,

$$\dot{e}(t)+\beta e(t)=0. \tag{4}$$

The solution of the equation given in (4) can be calculated as follow:

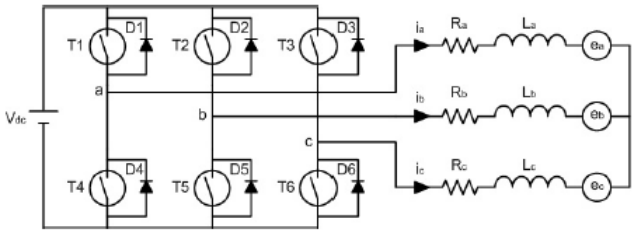

Figure 1. BLDCM Drive. [33]

$$e(t)=\bar{e}_0\,e^{-\beta t} \tag{5}$$

where $\bar{e}_0=\frac{1}{e_0}$ with a constant initial value e_0, it implies that

$$\int_0^t e(\tau)d\tau=\bar{e}_0\int_0^t e^{-\beta\tau}d\tau =-\bar{e}_0\beta e^{-\beta t}. \tag{6}$$

The proof is thus completed by the same decreasing rate value as that of $u(t)$.

3. Model of BLDCM Drives

In this section, the dynamical model of a three-phase BLDCM drive is presented. In the modeling of the BLDCM drive, some assumptions are taken into account as follows: (1) mutual inductance for each winding is zero, (2) resistances and inductances of three phases are equal, and (3) the neutral motor voltage is neglected. The equivalent circuit model of the BLDCM drive system is shown in Figure 1. The mathematical model of BLDC motor drive can be introduced as follows [34]:

$$L\frac{di_a(t)}{dt}=v_a(t)-Ri_a(t)-e_a(t) \tag{7}$$

$$L\frac{di_b(t)}{dt}=v_b(t)-Ri_b(t)-e_b(t) \tag{8}$$

$$L\frac{di_c(t)}{dt}=v_c(t)-Ri_c(t)-e_c(t) \tag{9}$$

where i_a,i_b,i_c denote the phase currents, v_a,v_b,v_c denote the phase voltages, e_a,e_b,e_c denote the back-EMF voltages, R is the resistance per phase and L is the inductance per phase. Besides, the following equality is satisfied:

$$i_a(t)+i_b(t)+i_c(t)=0. \tag{10}$$

The differential equation for the mechanical part of the BLDC motor drive is modeled as follows:

$$J\frac{d\omega(t)}{dt}=T_e(t)-T_l(t)-\beta\omega(t) \tag{11}$$

where J is the equivalent inertia, ω is the angular velocity of BLDC motor shaft, T_e is generated motor torque and T_l is the load torque. Besides, the motor output torque of the BLDCM can be formalized as follows:

$$T_e(t)=\frac{e_a(t)i_a(t)+e_b(t)i_b(t)+e_c(t)i_c(t)}{\omega(t)}. \tag{12}$$

To achieve the desired output torque, the BLDC motor types need a well-shaped current drive when it is considered the shape of back-EMF signals. However, driving the currents of the motor to

be obtained for each phase is not possible in practical applications. In practice, matched and un-matched uncertainties, external disturbances, faults in actuators, and nonlinearities also make the control of currents of the motor difficult. The main aim of this paper is to design a PI regulator for BLDC motor drives that takes the aforementioned drawbacks into account in the torque loop control. To facilitate the controller structure, the current dynamics given in (7)-(9) can be re-written as follows:

$$\frac{di_s(t)}{dt} = f(i_s, e_s) + g v_s(t) \tag{13}$$

where $= \{a, b, c\}$, $f(i_s, e_s) = -\frac{1}{L}Ri_s - \frac{1}{L}e_s$, $g = \frac{1}{L}$, and $v_s = \rho v + v_{un}$ with the definitions that ρ is actuator healthy rate, v is the controller input to be determined by the adaptive PI controller, v_{un} is uncontrollable part of the controller signal v_s given in (13). It is noticed that the controller gain g is a time-invariant unknown coefficient such that $0 \le \underline{g} \le |g| \le \overline{g}$, and ρ and v_{un} are unknown but bounded such that $0 < \underline{\rho} \le \rho \le 1$ and $|v_{un}| \le \overline{v}_{un}$ with unknown $\underline{\rho}$ and $\overline{v}_{un}$ values. Besides, the bounded uncertain function $f(i_s, e_s)$ includes the measurement of currents and back-EMF signals which render some nonlinear effects, and there exists an unknown time-invariant $f_c \ge 0$ and a known nonlinear function $\phi(i_s, e_s) \ge 0$ such that $|f(i_s, e_s)| \le f_c \phi(i_s, e_s)$.

4. Adaptive PI Controller

In this section, an adaptive PI controller is proposed for the torque loop control of BLDC motor drives, where the adaptive PI controller proposed in [26] is utilized for the regulation of the current of BLDCM drives to reduce the effects of the ripples over the output torque. It should be noted that the proposed controller is designed to address actuation failures, other uncertainties, and unknown controller gain. The designed controller diagram is presented in Figure 2.

First, the error expression can be defined as follows:

$$i_{es}(t) = i_s(t) - i_s^*(t) \tag{14}$$

where i_s^* is the desired sufficiently smooth current trajectory with $\frac{d^n i_s^*}{dt^n} \le \overline{i_s^*} \le \infty$. Then, the classical PI controller is

$$v(t) = -k_P i_{es}(t) - k_I \int_0^t i_{es}(\tau) d\tau \tag{15}$$

where k_P and k_I denote the non-negative PI controller gains, and the relationship of two controller gains can be assigned as $k_I = \beta k_P$ where the coefficient β is the controller design parameter. As it is given in (2), a filtered variable can be introduced as follows:

$$f_v(t) = i_{es}(t) + \beta \int_0^t i_{es}(\tau) d\tau. \tag{16}$$

The proposed controller structure is

$$v(t) = -(k_P + \Delta k_P(t)) i_{es}(t) - (k_I + \Delta k_I(t)) \int_0^t i_{es}(\tau) d\tau \tag{17}$$

where Δk_P and Δk_I are the time-varying controller gains to be determined by an adaptation rule, however, $\Delta k_I = \beta \Delta k_P$. Utilizing the filtered variable f_v given in (16), the proposed controller structure can be re-expressed as

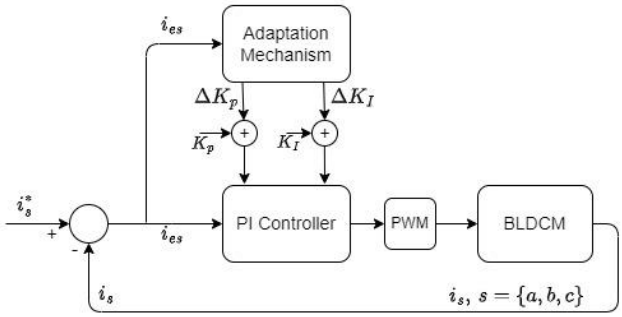

Figure 2. Block Diagram of the Adaptive PI Controller.

$$v(t) = -(k_P + \Delta k_P(t)) f_v(t) \tag{18}$$

Then, the derivation of the filtered variable is obtained as

$$\frac{df_v(t)}{dt} = f(i_s, e_s) + g\rho v(t) + g v_{un}(t) - \frac{di_s^*(t)}{dt} + \beta i_{es}(t) \tag{19}$$

and substituting (18) into (19), the equation (19) becomes

$$\frac{df_v(t)}{dt} = f(i_s, e_s) - g\rho(k_P + \Delta k_P(t)) f_v(t) + g v_{un}(t) - \frac{di_s^*(t)}{dt} + \beta i_{es}(t). \tag{20}$$

To be able to construct the adaptation rule and to analyze the stability of the system, we assume that the form of the estimation error is $\tilde{\theta}(t) = \theta - \gamma\hat{\theta}(t)$ where γ is a positive adaptation gain to be determined later, and the candidate Lyapunov function can be defined as

$$V(t) = \frac{1}{2} f_v^2(t) + \frac{1}{2\sigma \underline{g}\,\underline{\rho}} \tilde{\theta}^2(t) \tag{21}$$

whose derivative along the filtered trajectory of (16) is

$$\begin{aligned} \dot{V}(t) &= f_v(t) \frac{df_v(t)}{dt} + \frac{1}{\sigma \underline{g}\,\underline{\rho}} \tilde{\theta}(t) \frac{d\tilde{\theta}(t)}{dt} \\ &= f_v^2(t)\left(-g\rho(k_P + \Delta k_P(t))\right) + |f_v(t)|\Big(f(i_s, e_s) + g v_{un}(t) - \tfrac{di_s^*(t)}{dt} + \beta i_{es}(t)\Big) - \tfrac{\gamma}{\sigma \underline{g}\,\underline{\rho}} \tilde{\theta}(t) \tfrac{d\hat{\theta}(t)}{dt} \\ &\le f_v^2(t)\Big(-\underline{g}\,\underline{\rho}(k_P + \Delta k_P(t))\Big) + |f_v(t)|\big(f_c \phi(i_s, e_s) + \overline{g}\,\overline{v}_{un}(t) - \overline{i_s^*} + \beta |i_{es}(t)|\big) - \tfrac{\gamma}{\sigma \underline{g}\,\underline{\rho}} \tilde{\theta}(t) \tfrac{d\hat{\theta}(t)}{dt}. \end{aligned} \tag{22}$$

With the help of defining of $\theta = \max\{\overline{g}\,\overline{v}_{un} + \overline{i_s^*}, f_c, \beta\}$ and $\varphi(i_{es}, e_s) = 1 + \phi(i_s, e_s) + |i_{es}(t)|$, and time varying controller gain $\Delta k_P(t) = \frac{\hat{\theta}\,\varphi^2}{\varphi |f_v| + \epsilon}$, in which $\hat{\theta}(t)$ and ϵ stand for the estimation of the constant of θ and non-negative sufficiently small value respectively, the equation given in (22) becomes

$$\dot{V}(t) \le -\underline{g}\,\underline{\rho} k_P f_v^2(t) - \underline{g}\,\underline{\rho} \frac{\hat{\theta}(t) \varphi^2(i_{es}, e_s) f_v^2(t)}{\varphi(i_{es}, e_s) |f_v| + \epsilon} + \theta \varphi(i_{es}, e_s) |f_v(t)| - \frac{\gamma}{\sigma \underline{g}\,\underline{\rho}} \tilde{\theta}(t) \frac{d\hat{\theta}(t)}{dt}$$

$$\leq -\underline{g}\,\underline{\rho} k_P f_v^2(t) + \left(\theta - \underline{g}\,\underline{\rho}\hat{\theta}(t)\right)\left(\frac{\varphi^2(i_{es},e_s)f_v^2(t)}{\varphi(i_{es},e_s)|f_v|+\epsilon}\right) + \theta\epsilon - \frac{\gamma}{\sigma \underline{g}\,\underline{\rho}}\tilde{\theta}(t)\frac{d\hat{\theta}(t)}{dt} \quad (23)$$

where it is used $\frac{\varphi|f_v|}{\varphi|f_v|+\epsilon} \leq 1$ to obtain the right-hand side of (23). If the estimation error $\tilde{\theta}$ is re-defined as

$$\tilde{\theta}(t) = \theta - \underline{g}\,\underline{\rho}\hat{\theta}(t), \quad (24)$$

where $\underline{g}\,\underline{\rho} = \gamma$, then the inequality given in (23) turns into

$$\dot{V}(t) \leq -\gamma k_P f_v^2(t) + \tilde{\theta}(t)\left(\frac{\varphi^2(i_{es},e_s)f_v^2(t)}{\varphi(i_{es},e_s)|f_v|+\epsilon} - \frac{1}{\sigma}\frac{d\hat{\theta}(t)}{dt}\right) + \theta\epsilon. \quad (25)$$

The adaptation rule can be designed as follows:

$$\frac{d\hat{\theta}(t)}{dt} = -\sigma\kappa\hat{\theta}(t) + \sigma\frac{\varphi^2(i_{es},e_s)f_v^2(t)}{\varphi(i_{es},e_s)|f_v|+\epsilon} \quad (26)$$

where κ is a design parameter, and (25) transforms to

$$\dot{V}(t) \leq -\gamma k_P f_v^2(t) + \kappa\hat{\theta}(t)\tilde{\theta}(t) + \theta\epsilon \leq -\gamma k_P f_v^2(t) - \frac{\kappa}{2\gamma}\left(\tilde{\theta}^2(t) - \theta^2\right) + \theta\epsilon \quad (27)$$

where $\hat{\theta}(t)\tilde{\theta}(t) = \frac{1}{\gamma}\left(\theta - \tilde{\theta}(t)\right)\tilde{\theta}(t) \leq \frac{1}{2\gamma}\left(\theta^2 - \tilde{\theta}^2(t)\right)$ is employed by using inequality $2\theta\tilde{\theta}(t) \leq \theta^2 + \tilde{\theta}^2(t)$. Thus,

$$\dot{V}(t) \leq -\gamma k_P f_v^2(t) - \frac{\kappa}{2\gamma}\left(\tilde{\theta}^2(t) - \theta^2\right) + \theta\epsilon \leq -\delta_1 V(t) + \delta_2 \quad (28)$$

where $\delta_1 = \min\{2k_P\gamma, \kappa\} > 0$ and $\delta_2 = \frac{\kappa}{2\gamma}\theta^2 + \theta\epsilon$. The solving of $\dot{V} \leq -\delta_1 V + \delta_2$ is $V \leq \frac{\delta_2}{\delta_1} + \left(V(0) - \frac{\delta_2}{\delta_1}\right)e^{-\delta_1 t}$ which implies that all signals of the current dynamics of BLDCM drive system are uniformly ultimately bounded (UUB) with the globally attractive set $S = \left\{(f_v, \tilde{\theta})\middle| V \leq \frac{\delta_2}{\delta_1}\right\}$. According to Lemma 2.2, the error variable f_v is also UUB. The filtered variable satisfies $|f_v| \leq \sqrt{2\frac{\delta_2}{\delta_1}}$ which means the filtered variable is bounded in a finite time. Hence, the filtered variable converges to a very small neighborhood of origin, and the convergence rate can be tuned by appropriate parameters mentioned in the stability analysis. Moreover, i_{es} and $\int_0^t i_{es}(\tau)d\tau$ are continuous and bounded according to Lemma 2.2, and the value of $\frac{\delta_2}{\delta_1}$ is related to the design parameters, so the error i_{es} converges to a very small neighborhood of origin.

5. Simulation Results

Several numerical simulations have been carried out to assess the performance of the proposed adaptive PI controller. Implementation of the simulation has been done on MATLAB/Simulink. The back-EMF signals are considered to be ideal. Phase inductance and phase resistance of the BLDC are taken as $L = 2.5\ mH$ and $R = 0.58\ \Omega$. Three-phase inverter is fed by a DC voltage source of 48V. PWM is created with the switching frequency of 10kHz and there is no switching loss since the switches are ideal. For the first part of the comparisons, PI controller parameters are chosen as $k_p = 2$, $\beta = 1$, where $k_I = \beta k_p$. Adaptation parameters are assigned $\sigma = 10000$, $\kappa = 0.01$ and $\epsilon = 0.001$. Rotor speed is taken constant throughout the simulations. For the second part of the comparisons, the proposed adaptive PI controller is compared to a high-gain controller, where $k_h = 10, \beta_h = 21.2$ and $\epsilon_h = 10$, to solidify the performance of the proposed adaptive PI controller. The design steps of the high gain controller are given in Appendix.

Miscellaneous numerical simulations have been carried out for different references and rotor speeds. In the first comparison, each simulation results are illustrated with a duration of 0.1s. Adaptive PI controller does not take place in the first half of the simulations. In the second half, adaptation rules apply to the PI controller. Figure 3 and Figure 4 illustrate the results for constant and sinusoidal current reference at 500rpm constant rotor speed.

In these numerical results, each current, the error of currents, the controller input, the generated motor torque, the estimation parameter $\hat{\theta}$ and time-varying proportional controller gain are presented, respectively. Table 1 and Table 2 represent the numerical values, which were obtained from the simulations that are illustrated in Figure 3 – Figure 6. As illustrated in Figure 3 - Figure 6, the error presence is significant with conventional PI at lower and higher speeds both for constant and sinusoidal reference. However, as the adaptive PI is applied, the steady-state error is significantly compensated and the ripple widths in current, and error in torque response are decreased. Besides, it is also proved that the internal signals are converging to a constant value, as shown by the means of Lyapunov theory in Section 4. Table 1 and Table 2 demonstrate that with the proposed adaptive PI controller, the RMS value of the current error for constant current reference has been improved from 0.3442 to 0.0656 at 500rpm, and from 0.4703 to 0.1552 at 1500rpm. The RMS value of the current error for sinusoidal current reference has been improved from 0.3432 to 0.0670 at 500rpm, and from 0.4700 to 0.1677 at 1500rpm. Overall, the current error RMS value has improved by approximately 60% - 80% at high and low speeds, respectively. Additionally, the current error has been improved by around 7% during commutation period. It stands out that the control signal in both constant and sinusoidal current reference changes significantly as adaptive PI controller kicks in, as opposed to the conventional PI controller. This is due to the controller design parameters, especially sufficiently small ϵ value having significant effect on the magnitude of the control signals, which can be deduced from the adaptation rule given in (26).

In the second comparison, in the first half of the simulation, the proposed adaptive PI controller does not take place and a high-gain controller is utilized to regulate the system. In the second half of the simulation, the proposed adaptive PI controller takes place. Figure 7 and Figure 8 illustrate the comparison of high-gain controller and adaptive PI controller with constant and sinusoidal current reference at 1500rpm constant rotor speed. In these numerical results, each current, the error of currents, the controller input are presented, respectively. Additionally, in this case, small ϵ value is increased to 0.1 to observe the effects on control signal and the reference tracking performance. In Figure 7 and Figure 8, it is obvious that with the high-gain controller, the reference tracking performance has significantly increased compared to the first case. However, even the maximum value of the current response with high-gain controller is still under the current reference value, namely it still exists steady state error. Also, the control signal of high-gain controller has increased. In the second half of the simulation, proposed adaptive PI controller is applied. When adaptive PI is applied, the current response swiftly sits on the current reference value, outperforming the high-gain controller. It is also obvious that by increasing the small

ϵ value, the control input of the adaptive PI controller decreased significantly. Moreover, it even is smaller in magnitude compared to the high-gain controller, meaning that the proposed adaptive PI controller achieves better current response with less energy consumption in control input. In Table 3 and Table 4 numerical values, which were obtained from the simulations that are illustrated in Figure 7 and Figure 8, are represented. With the proposed method the RMS value of the current error has improved from 0.1853 to 0.1611 with constant current reference at 1500rpm. With sinusoidal current reference at 1500rpm, the RMS value of the current error has been improved from 0.1879 to 0.1720. Overall, the RMS of the current response and current error have been improved by approximately 9%. In addition to that, the designed controller seems to be a high-gain controller but it is a controller that consumes less energy and responds easily to a non-linear changing system. We especially see this phenomenon in the switching case of the system, which is due to that the adaptation in the designed controller is updated according to the system dynamics.

Consequently, numerical solutions solidify the success of the proposed adaptive PI controller on BLDCM drives by employing comparisons with a conventional PI controller and a high-gain controller, while ensuring the stability of the controller by Lyapunov theory and the ability to compensate for the effects of external disturbances, nonlinearities, and uncertainties.

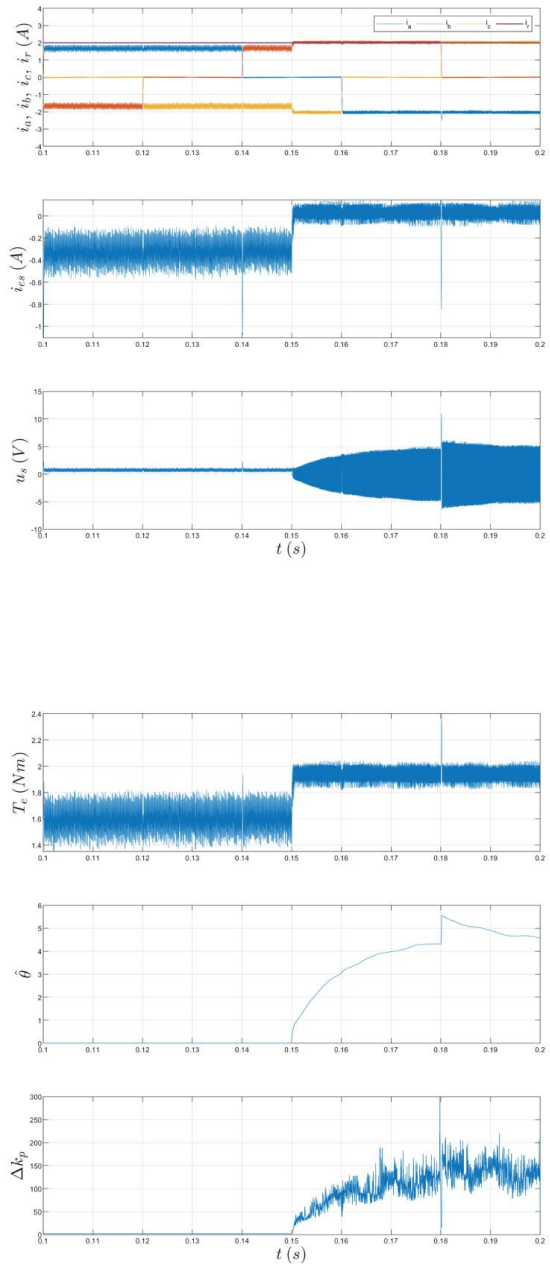

Figure 3. Simulation results for 2A constant current reference at 500 rpm constant speed. Change of the phase currents, current error, control input, torque, estimation of θ, and adaptation gain Δk_p, respectively from top to bottom.

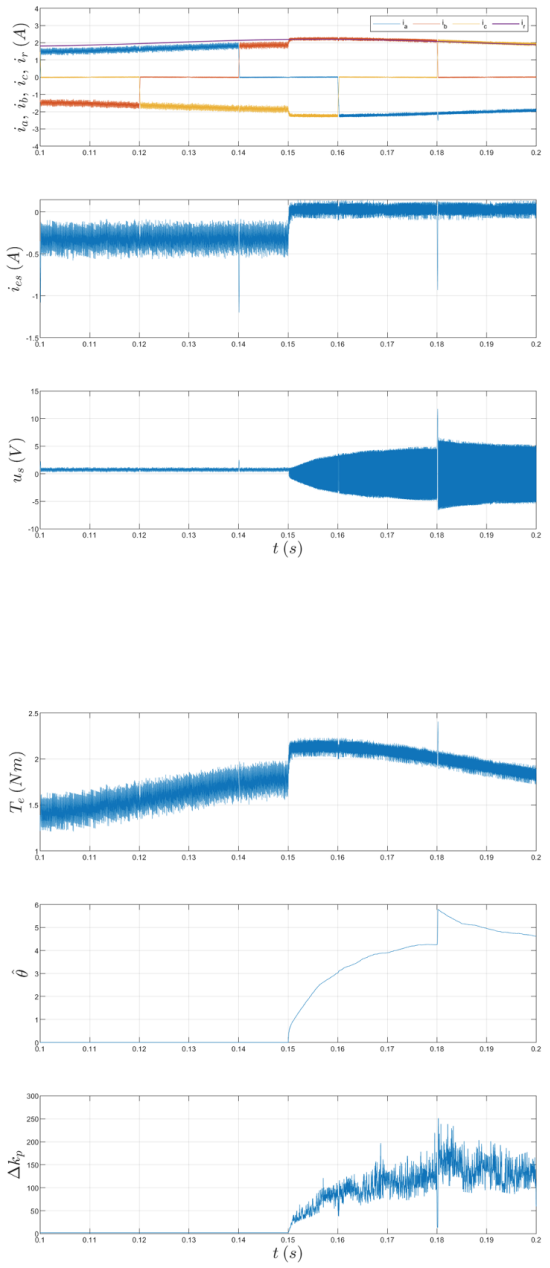

Figure 4. Simulation results for sinusoidal current reference at 500rpm constant speed. Change of the phase currents, current error, control input, torque, estimation of θ, and adaptation gain Δk_p, respectively from top to bottom.

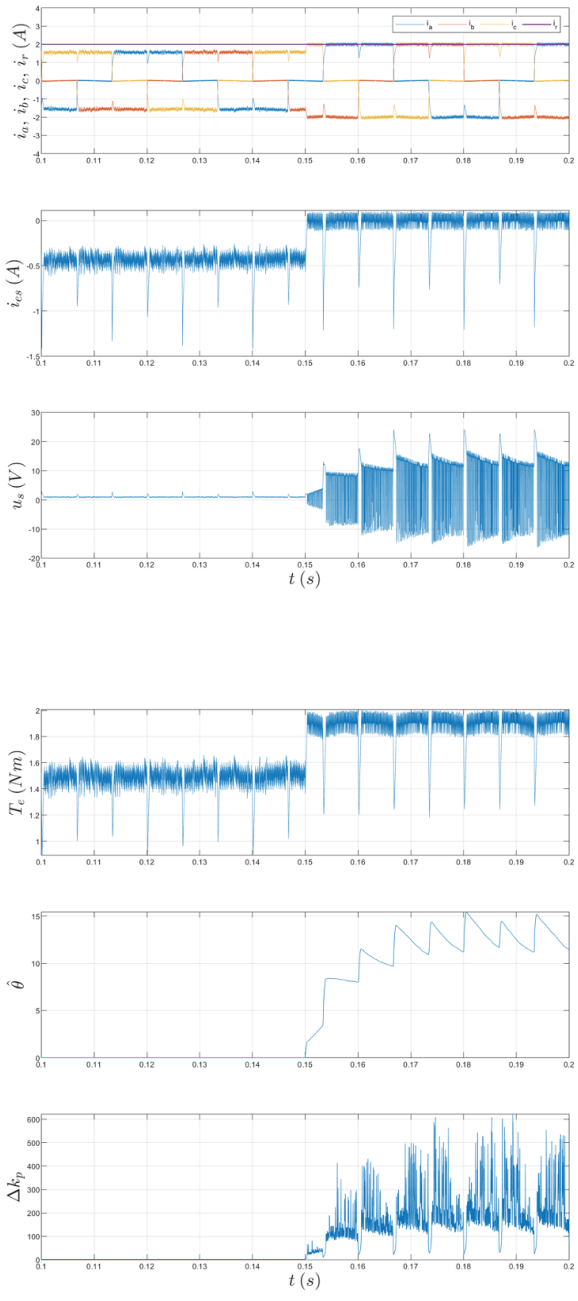

Figure 5. Simulation results for 2A constant current reference at 1500rpm constant speed. Change of the phase currents, current error, control input, torque, estimation of θ, and adaptation gain Δk_p, respectively from top to bottom.

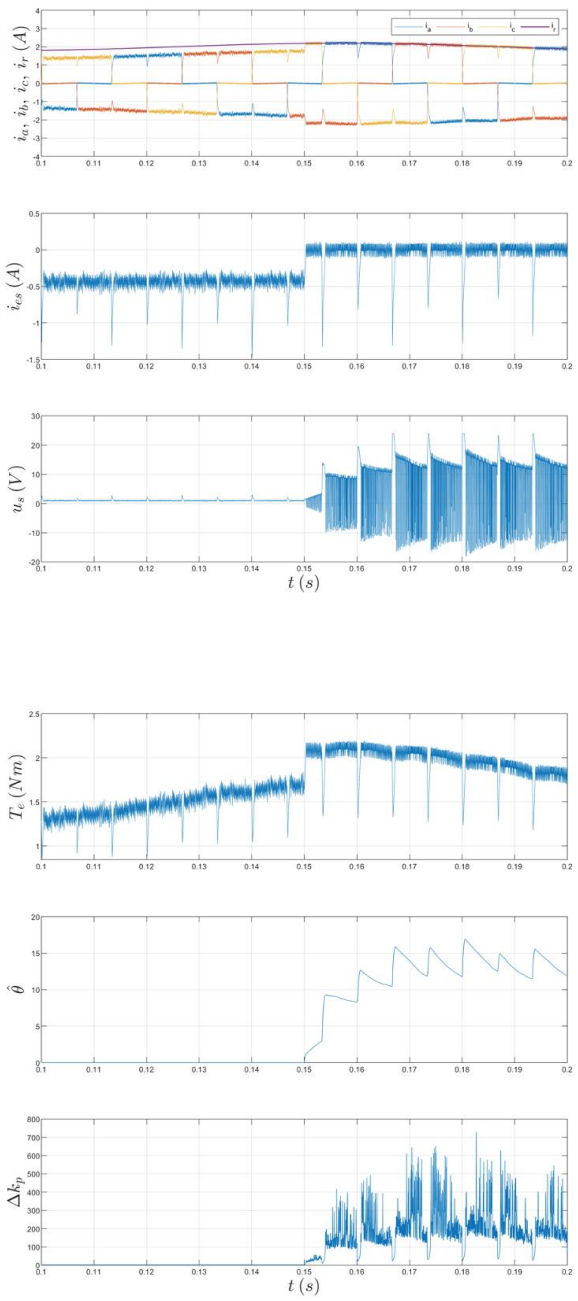

Figure 6. Simulation results for sinusoidal current reference at 1500rpm constant speed. Change of the phase currents, current error, control input, torque, estimation of θ, and adaptation gain Δk_p, respectively from top to bottom.

Table 1. Numerical simulation results for 2A constant current reference at different speeds.

	ω	$i_{s_{rms}}$	$i_{es_{rms}}$
Classical PI	500rpm	1.6757	0.3442
Adaptive PI	500rpm	2.0267	0.0656
Classical PI	1500rpm	1.5487	0.4703
Adaptive PI	1500rpm	1.9718	0.1552

Table 2. Numerical simulation results for sinusoidal current reference at different speeds.

	ω	$i_{s_{rms}}$	$i_{es_{rms}}$
Classical PI	500rpm	1.6818	0.3432
Adaptive PI	500rpm	2.1178	0.0670
Classical PI	1500rpm	1.5539	0.4700
Adaptive PI	1500rpm	2.0601	0.1677

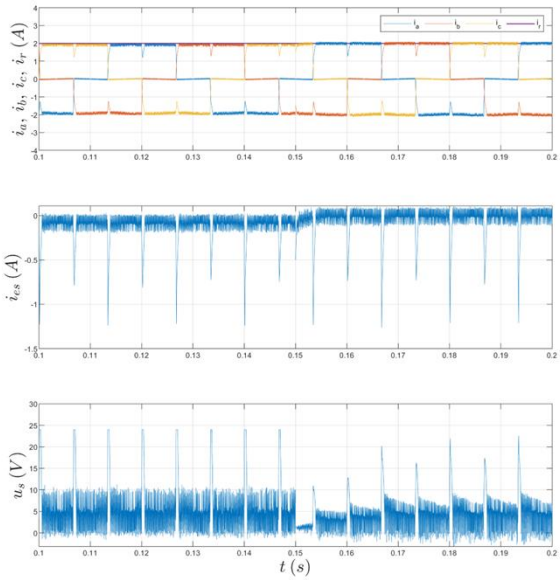

Figure 7. Simulation results of comparison of high-gain controller and adaptive PI for 2A constant current reference at 1500rpm constant speed. Change of the phase currents, current error, control input, respectively from top to bottom.

Table 3. Numerical simulation results of comparison of high-gain controller and adaptive PI for 2A constant current reference.

	ω	$i_{s_{rms}}$	$i_{es_{rms}}$
High-gain Controller	1500rpm	1.8915	0.1853
Adaptive PI	1500rpm	1.9628	0.1611

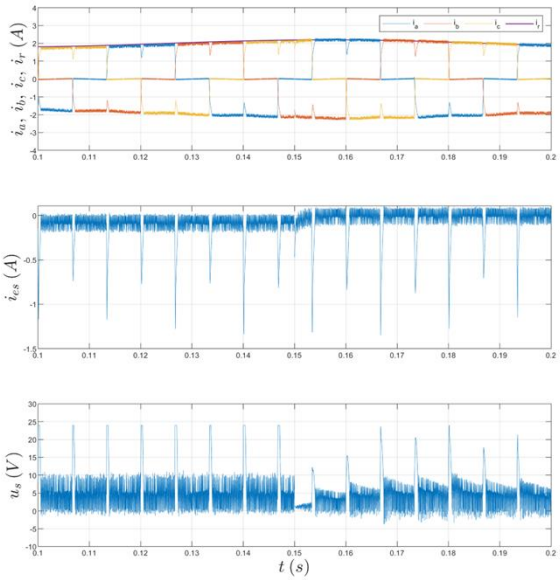

Figure 8. Simulation results of comparison of high-gain controller and adaptive PI for sinusoidal current reference at 1500rpm constant speed. Change of the phase currents, current error, control input, respectively from top to bottom.

Table 4. Numerical simulation results of comparison of high-gain controller and adaptive PI for sinusoidal current reference.

	ω	$i_{s_{rms}}$	$i_{es_{rms}}$
High-gain Controller	1500rpm	1.8938	0.1879
Adaptive PI	1500rpm	2.0515	0.1720

6. Conclusions

This paper proposes an adaptive PI controller for the regulation of currents in the torque loop of BLDCM drives. The proposed controller guarantees that all signals in the closed-loop dynamics remain bounded. Additionally, the trajectory tracking error of the currents tends to a very small neighborhood of the origin, which can be tuned by the adaptation rule. The convergence rate is adjusted with a pre-defined constant decreasing rate with the filtered variable. The proposed controller is tested with numerical simulations containing simulations that address nearly all practical issues, along with comparisons to the classical PI controller. When the PI controller is compared with the designed adaptive control, a better response in the regulation of currents of BLDCM observed a reduction in the root mean square (RMS) error current by 35.57% for a sinusoidal current reference at 1500 rpm when compared to the PI controller. In comparison, the reduction rate observed with the high-gain controller is approximately 9%. Future studies plan to extend the presented controller design to the torque loop of variable-speed brushless DC motor drives and implement the proposed controller in real-time on a BLDCM driver.

Appendix

In Appendix, the design steps of a high-gain nonlinear current controller based on Lyapunov function is presented to facilitate the comparative analysis.

First, the error expression can be re-defined as follows:

$$i_{es}(t) = i_s(t) - i_s^*(t) \tag{A-1}$$

where i_s^* is the desired sufficiently smooth current trajectory. Utilizing the equation (13), the current error dynamic is obtained as follows:

$$\frac{1}{g}\frac{di_{es}(t)}{dt} = \frac{f(i_s, e_s)}{g} + v_s(t) - \frac{1}{g}\frac{di_s^*(t)}{dt} \tag{A-2}$$

where the notations are defined in Section 3, and we assume that $0 \leq \frac{f(i_s,e_s)}{g} - \frac{1}{g}\frac{di_s^*(t)}{dt} \leq \beta_h$. In order to design a high-gain controller, we consider the following candidate Lyapunov function:

$$V(t) = \frac{1}{2g} {i_{es}}^2(t). \tag{A-3}$$

If the derivation of $V(t)$ with the respect to time is taken, it gives as follows:

$$\frac{dV(t)}{dt} = i_{es}(t)\left(\frac{f(i_s, e_s)}{g} + v_s(t) - \frac{1}{g}\frac{di_s^*(t)}{dt}\right). \tag{A-4}$$

Considering the equation (A-4), the controller input can be designed as:

$$v_s(t) = -k_h i_{es}(t) - \frac{\beta_h^2\, i_{es}(t)}{\epsilon_h}, \quad \epsilon_h > 0. \tag{A-5}$$

After the controller input given in (A-5) is proposed, the equation (A-4) turns into

$$\begin{aligned}\frac{dV(t)}{dt} &= -k_h i_{es}^2(t) - \frac{\beta_h^2\, i_{es}^2(t)}{\epsilon_h} + \frac{f(i_s, e_s)}{g} - \frac{1}{g}\frac{di_s^*(t)}{dt} \\ &\leq -k_h i_{es}^2(t) - \frac{\beta_h^2\, i_{es}^2(t)}{\epsilon_h} + \beta_h |i_{es}(t)| \\ &= -k_h i_{es}^2(t) + \beta_h |i_{es}(t)| \left(1 - \frac{\beta_h\, |i_{es}(t)|}{\epsilon_h}\right)\end{aligned} \tag{A-6}$$

where if $\beta_h |i_{es}(t)| \geq \epsilon_h$, then $\frac{dV(t)}{dt} \leq -k_h i_{es}^2(t)$ which means that $i_{es}(t)$ converges to zero. It is noticed that this case is satisfied under the condition of sufficiently high values of $\beta_h |i_{es}(t)|$.

Ethics committee approval and conflict of interest statement

This article does not require ethics committee approval. This article has no conflicts of interest with any individual or institution.

Acknowledgment

As authors, we are grateful to the Editor and three anonymous reviewers for their comments and suggestions, which contributed significantly to the improvement of the manuscript.

This article is part of the under-graduate thesis of C. Arslanoğlu (corresponding author).

Author Contribution Statement

Author 1 (corresponding author) conducted the literature review, wrote the manuscript focusing on conceptualization and results presentation, and developed and implemented the simulation works used in this article. Author 2 contributed to conduct the literature review, provided key insights for the paper's theoretical framework, contributed to writing and editing processes, and conducted a critical review offering feedback for improvement.

References

[1] Xia, C.-l. 2012. Permanent Magnet Brushless DC Motor Drives and Controls, John Wiley & Sons Singapore Pte. Ltd., 282s.

[2] Krishnan, R. 2009. Permanent Magnet Synchronous and Brushless DC Motor Drives, Taylor and Francis Group, LLC, 584s.

[3] Hemati, N., Leu, M. C. 1992. A complete model characterization of brushless DC motors, IEEE Transactions on Industry Applications, Vol. 28, p. 172-180, DOI: 10.1109/28.120227

[4] Sharma, P. K., Sindekar, A. S. 2016. Performance analysis and comparison of BLDC motor drive using PI and FOC, 2016 International Conference on Global Trends in Signal Processing, Information Computing and Communication (ICGTSPICC), Jalgaon, India, pp. 485-492.

[5] Hari, K. U., Rajeevan, P. P. 2022. A Direct Torque Control Scheme for BLDC Motor Drives with Open-end Windings, 2022 IEEE 1st Industrial Electronics Society Annual On-Line Conference (ONCON), Kharagpur, India, 1-6.

[6] İnan, R., Üzüm, O. M. 2022. Speed-Sensorless DTC of BLDC Motor with EKF-based Estimator Capable of Load Torque Estimation for Electric Vehicle. Avrupa Bilim Ve Teknoloji Dergisi, Vol.42, pp. 6-13. DOI: 10.31590/ejosat.1190197

[7] Ubare, P., Ingole, D., Sonawane, D.N. 2021. Nonlinear Model Predictive Control of BLDC Motor with State Estimation, IFAC-PapersOnLine, Vol. 54, pp. 107-112. DOI: 10.1016/j.ifacol.2021.08.531

[8] Ramesh, P., Ranjeev, A., Santhakumar, C., Vinoth, J., Bharatiraja, C. 2022. Sensor-less field orientation control for brushless direct current motor controller for electric vehicles, Materials Today: Proceedings, Vol. 65, pp. 277-284, DOI: 10.1016/j.matpr.2022.06.168

[9] Soni, U. K., Tripathi, R. K. 2017, Novel back EMF zero difference point detection based sensorless technique for BLDC motor, 2017 IEEE International Conference on Industrial Technology (ICIT), Toronto, ON, Canada, pp. 330-335

[10] John, M., Thomas, V. 2014. Position sensorless control of BLDC motor based on back EMF difference estimation method, 2014 Power And Energy Systems: Towards Sustainable Energy, Bangalore, India, pp. 1-6, DOI: 10.1109/pestse.2014.6805283

[11] Chowdhury, D., Chattopadhyay, M., Roy, P. 2013. Modelling and Simulation of Cost Effective Sensorless Drive for Brushless DC Motor, Procedia Technology, Vol. 10, pp. 279-286, DOI: 10.1016/j.protcy.2013.12.362

[12] Kalyani, S. T., Md, S. K. 2013. Simulation of sensorless operation of BLDC motor based on the zero-cross detection from the line voltage, International Journal of Advanced Research in Electrical, Electronics and Instrumentation Engineering, Vol.. 2, pp. 6185-619.

[13] Visoli, A., 2006. Practical PID Control, London: Springer-Verlag.

[14] Song, Y.D. 2018. Control of Nonlinear System via PI, PD and PID: Stability and Performance, CRC Press/Taylor & Francis Group.

[15] Türker, T. 2018. Fırçasız doğru akım motorunun hız kontrolü için uyarlamalı geri adımlamalı kontrolcü tasarımı, Pamukkale Üniversitesi Mühendislik Bilimleri Dergisi, Vol. 24, pp. 214–218, DOI: 10.5505/pajes.2017.72623

[16] Mamadapur, A., Unde Mahadev, G. 2019. Speed Control of BLDC Motor Using Neural Network Controller and PID Controller, 2nd International Conference on Power and Embedded Drive Control (ICPEDC), Chennai, India, pp. 146-151.

[17] Moradi, M., Ahmadi, A., Abhari, S. 2010. Optimal control based feedback linearization for position control of DC motor, 2nd International Conference on Advanced Computer Control, Shenyang, China, pp. 312-316.

[18] Shirvani Boroujeni, M., Arab Markadeh, G. Soltani, J. 2017. Adaptive Input-output feedback linearization control of Brushless DC Motor with arbitrary current reference using Voltage Source Inverter, 8th Power Electronics, Drive Systems & Technologies Conference (PEDSTC), Mashhad, Iran, pp. 537-542.

[19] Awadallah, M., Bayoumi, E., Soliman, H. 2009. Adaptive deadbeat controllers for brushless DC drives using PSO and ANFIS techniques. Journal of Electrical Engineering. Vol. 60, pp. 3-11.

[20] Baz, R., Majdoub, K. E., Giri, F., Taouni, A. 2022. Self-tuning fuzzy PID speed controller for quarter electric vehicle driven by In-wheel BLDC motor and Pacejka's tire model, IFAC-PapersOnLine, Vol. 55, pp.598-603, DOI: 10.1016/j.ifacol.2022.07.377

[21] Umam, M. K. Hasanah, R. N., Nurwati, T. 2022. PID-based Fuzzy Logic Theory Implementation on BLDC Motor Speed Control, 2022 International Seminar on Intelligent Technology and Its Applications (ISITIA), Surabaya, Indonesia, pp. 407-412.

[22] Kumar, B. H., Bhimasingu, R., Kumar, V. S. S. 2022. Fuzzy-PI based model predictive control for speed control of BLDC motor, 2022 IEEE International Conference on Power Electronics, Drives and Energy Systems (PEDES), Jaipur, India, pp. 1-6.

[23] Shahnazi, R., M. Akbarzadeh-T., R. 2008. PI Adaptive Fuzzy Control with Large and Fast Disturbance Rejection for a Class of Uncertain Nonlinear Systems, IEEE Transactions on Fuzzy Systems, Vol. 16, pp. 187-197, DOI: 10.1109/tfuzz.2007.903320

[24] Chang, W., Hwang, R., Hsieh, J. 2022. A self-tuning PID control for a class of nonlinear systems based on the Lyapunov approach, Journal of Process Control, Vol.12, pp. 233-242, DOI: 10.1016/s0959-1524(01)00041-5

[25] Song, Q., Song, Y.D. 2014. Generalized PI control design for a class of unknown nonaffine systems with sensor and actuator faults, Systems & Control Letters, v. 64, p. 86-95, DOI: 10.1016/j.sysconle.2013.11.011

[26] Y. Song, Y. Wang and C. Wen, "Adaptive Fault-Tolerant PI Tracking Control With Guaranteed Transient and Steady-State Performance," in IEEE Transactions on Automatic Control, Vol. 62, no. 1, pp. 481-487, Jan. 2017, DOI: 10.1109/TAC.2016.2554362.

[27] Song, Y. Huang, X. Wen, C. 2017. Robust Adaptive Fault-Tolerant PID Control of MIMO Nonlinear Systems With Unknown Control Direction, IEEE Transactions on Industrial Electronics, v. 64, p. 4876-4884, DOI: 10.1109/tie.2017.2669891

[28] Shi, J. Li, T., C. 2013. New Method to Eliminate Commutation Torque Ripple of Brushless DC Motor With Minimum Commutation Time, IEEE Transactions on Industrial Electronics, Vol. 60, pp. 2139-2146, DOI: 10.1109/tie.2012.2191756

[29] Lin, Y. -K., Lai, Y. S. 2011. Pulsewidth Modulation Technique for BLDCM Drives to Reduce Commutation Torque Ripple Without Calculation of Commutation Time, IEEE Transactions on Industry Applications, Vol. 47, pp. 1786-1793, DOI: 10.1109/tia.2011.2155612

[30] Türker, T. and Khudhair, I., O., K. 2017. A switched current controller with commutation delay compensation for the reduction of commutation torque ripple in BLDCM drives, Turkish Journal of

Electrical Engineering and Computer Sciences: Vol. 25, pp. 2635-2646 DOI: 10.3906/elk-1606-105

[31] Adıgüzel, F. Türker, T. 2017. A switching adaptive controller for the reduction of commutation torque ripple in BLDCM drives, 10th International Conference on Electrical and Electronics Engineering (ELECO), Bursa, Turkey, pp. 244-248.

[32] Haddad, W., M., VijaySekhar, C. 2008, Nonlinear Dynamical Systems and Control, Princeton University Press.

[33] Adıgüzel, F., Türker, T. 2022. A periodic adaptive controller for the torque loop of variable speed brushless DC motor drives with non-ideal back-electromotive force, Automatika, Vol.63:4, pp. 732-744, DOI: 10.1080/00051144.2022.2065802

[34] Adıgüzel, F., Türker, T. 2017. A switching adaptive current controller for BLDCM drives, 21st International Conference on System Theory, Control and Computing (ICSTCC), Sinaia, Romania, pp. 334-339.